Journal of Applied Fluid Mechanics, Vol. 9, No. 6, pp. 2877-2885, 2016.
Available online at www.jafmonline.net, ISSN 1735-3572, EISSN 1735-3645.

Chemical Reaction Effects on an Unsteady MHD Mixed Convective and Radiative Boundary Layer Flow over a Circular Cylinder

T. Poornima[1†], P. Sreenivasulu[2] and N. Bhaskar Reddy[3]

[1] *Department of Mathematics (SAS),VIT University, Chennai-600127, India.*
[2]*Department of Mathematics (HAS), SVCET, Chittoor-517127,AP, India.*
[3]*Department of Mathematics,Sri Venkateswara University, Tirupati-517502,Ap,India.*

†*Corresponding Author Email: poonima.anand@gmail.com*

(Received November 24, 2014; accepted November 2, 2015)

ABSTRACT

A mathematical model is presented for an optically dense fluid past an isothermal circular cylinder with chemical reaction taking place in it. A constant, static, magnetic field is applied transverse to the cylinder surface. The cylinder surface is maintained at a constant temperature. New variables are introduced to transform the complex geometry into a simple shape and the boundary layer conservation equations, which are parabolic in nature, are normalized into non-similar form and then solved numerically with the well-tested, efficient, implicit, Crank-Nicolson finite difference scheme. Numerical computations are made and the effects of the various material parameters on the velocity, temperature and concentration as well as the surface skin friction and surface heat and mass transfer rates are illustrated graphs and tables. Increasing magnetohydrodynamic body force parameter (M) is found to decelerate the flow but enhance temperatures. Thermal radiation is seen to reduce both velocity and temperature in the boundary layer. Local Nusselt number is also found to be enhanced with increasing radiation parameter.

Keywords: Circular cylinder; Chemical reaction; Magnetohydrodynamics; Heat and mass transfer; Unsteady flow.

NOMENCLATURE

A	radius of cylinder
B_0	magnetic induction
C	species concentration at the of the fluid in boundary layer
C_P	specific heat at constant pressure
C_w	concentration of the surface of the cylinder
D	species diffusion coefficient
Gc	solutal Grashof number
Gr	thermal Grashof number
g	acceleration due o gravity
k	thermal conductivity of the fluid
k^*	mean absorption coefficient
M	magnetic parameter
N	buoyancy ratio parameter
Nr	radiation parameter
Pr	Prandtl number
q_r	radiative heat flux
R	radiation parameter
Sc	Schmidt number
T	Fluid temperature.
T_0	reference temperature
T_w	surface temperature
T_∞	variable ambient temperature
t'	time
u', v'	velocity components in x', y' directions
α	thermal diffusivity
β and β^*	volumetric coefficient of thermal and solutal expansions
ν	kinematic viscosity
ρ	fluid density
μ	coefficient of fluid viscosity
σ	electrical conductivity
σ_e	Stephen Boltzmann constant
η	similarity variable
θ	non-dimensional temperature
ϕ	non-dimensional concentration

Subscripts

w	conditions on the wall
∞	free stream conditions
i	designates the grid point along the X-direction
j	grid point along Y- direction
n	along the t-direction

1. INTRODUCTION

From an industrial point of view, the study of thermal radiation effects on free convective magnetohydrodynamic (MHD) flows, has gained more importance in recent years. Many processes in engineering phenomena occur at high temperatures and the knowledge of radiation heat transfer has become very significant for the design of pertinent equipment at these temperatures. Several theoretical and experimental investigations on heat and mass transfer characteristics, radiation effects and free convection have been carried out from the beginning of sixties. The radiation effect on heat transfer along stretching surface has first been reported by Elbashbeshy (2000). Recently, Ghaly and Elbarbary (2000) investigated the radiation effect on MHD free convective flow of a gas at a stretching surface with a uniform free stream. Seddeek (2001) studied thermal radiation and buoyancy effects on MHD free convective heat generated flow over an accelerating permeable surface with temperature dependent viscosity. Aboeldahab and Seddeek (2001) studied the radiation and Hall current effects on an unsteady MHD free convection near an infinite vertical porous plate. Hossain *et al.* (1999) studied the radiation interaction on combined forced and free convection across a horizontal cylinder. Hakiem *et al*. (2007) analyzed the effect of radiation on non-Darcy free convection from a vertical cylinder embedded in a fluid-saturated porous medium with a temperature-dependent viscosity. Molla *et al*. (2011) examined the radiation effects on natural convection laminar flow from a horizontal circular cylinder. Uddin and Manoj Kumar (2011) investigated the effects of thermal radiation on MHD heat and mass transfer free convection flow near the lower stagnation point of an isothermal cylinder imbedded in porous domain. Loganathan *et al*. (2011) studied the thermal radiation effects on MHD flow over a moving semi-infinite vertical cylinder. Elbashbeshy and Aldawody (2011) analyzed the radiation effects on unsteady MHD mixed convection flow and heat transfer over a porous stretching surface in the presence of internal heat generation/absorption. Duwair (2006) discussed the thermal radiation effects on mixed convection over a non-isothermal cylinder and sphere in a porous media.

Bhuiyan *et al.* (2014) studied the Joule heating effects on MHD natural convection flows in presence of pressure stress work and viscous dissipation from a horizontal circular cylinder. Recently Sreenivasulu and Bhaskar Reddy (2015), investigated the Lie Group analysis for boundary layer flow of nanofluids near the stagnation-point over a permeable stretching surface embedded in a porous medium in the presence of radiation and heat generation/absorption. Das *et al.* (2015) presented the unsteady free convection flow past a vertical plate with heat and mass fluxes in the presence of thermal radiation.

In many chemical engineering processes there is a chemical reaction between a foreign mass and a fluid. These processes take place in numerous industrial applications such as manufacturing of ceramics, food processing and polymer production. The effects of mass transfer on the flow past an impulsively started infinite vertical plate under constant heat flux condition along with chemical reaction were studied by Das *et al.* (1994). Ganesan and Loganathan (2002) studied free convection boundary layer flow of a viscous and incompressible fluid past an impulsively started semi-infinite vertical cylinder with uniform heat and mass fluxes and chemically reactive species. They obtained the numerical solutions by the finite-difference scheme of Crank-Nicolson type. The effect of diffusion of chemically reactive species in convective flow along a vertical cylinder has been investigated by Ganesan and Rani (2000).The authors discussed the Nusselt number, Sherwood number for both generative and destructive reaction cases. Muthucumaraswamy and Shankar (2004) studied the first order chemical reaction effects on an unsteady flow past a uniformly accelerated isothermal infinite vertical plate with heat and mass transfer in the presence of thermal radiation. The interaction of free convection with thermal radiation of a viscous incompressible unsteady flow past a moving vertical cylinder with heat and mass transfer is analyzed by Ganesan and Loganathan (2005). Transient free convection about vertical plates and circular cylinders was studied by Goldstein and Briggs (1964). Hye *et al.* (2007) explained the combined heat and mass transfer effects on natural convection flow across an isothermal horizontal circular cylinder with chemical reaction. Shit and Majee (2014) studied the hydromagnetic flow over an inclined non-linear stretching sheet with variable viscosity in the presence of thermal radiation and chemical reaction.

In view of the above observations, in the present chapter, an attempt is made to study the heat and mass transfer effects on a mixed convection flow of a viscous incompressible electrically conducting, radiating and chemically reacting fluid along a horizontal circular cylinder. New variables to transform the complex geometry into a simple shape have been introduced and the resulting non-similarity boundary layer equations are solved by a very efficient implicit finite difference method together with Crank- Nicolson scheme. The influence of various governing physical parameters on the velocity, temperature, concentration as well as the skin-friction, Nusselt number and Sherwood number have been computed numerically and discussed in detail.

2. MATHEMATICAL ANALYSIS

Consider an unsteady two-dimensional laminar mixed convective flow over a horizontal circular cylinder of radius a, which is immersed in a viscous and incompressible fluid is considered. The x - coordinate is measured along the circumference of the horizontal cylinder and the y - coordinate is measured normal to the surface, with 'a' denoting the radius of the horizontal cylinder. The fluid is assumed to be gray, absorbing-emitting but non-

scattering. Initially, it is assumed that the surface of the cylinder and the fluid are at the same temperature T'_∞ and concentration level C'_∞ everywhere in the fluid. At time $t' > 0$, the temperature of the surface and the concentration level near the surface are raised to T'_w and C'_w respectively and are maintained constantly thereafter. The configuration of the flow field is shown in the following Figure. An appropriate mass transfer analogue to the problem shown in the above figure would be the flow across the surface of a horizontal circular cylinder that contains a species A slightly soluble in the fluid B. The concentration of the reactant is maintained at a constant value C_w at the surface of the cylinder and the solubility of A in B is D and the concentration of A far away from the surface of the cylinder is assumed to be C_∞. It is assumed that there is a first order homogeneous chemical reaction between the species A and the fluid B, with rate constant, K_1. It is assumed that the concentration of dissolved species A is small enough and the physical properties of ρ, μ and D are virtually constant throughout the fluid.

A uniform magnetic field is applied transversely to the direction of the flow. The transverse applied magnetic field and magnetic Reynolds number are assumed to be very small, so that the induced magnetic field is negligible. It is assumed that the concentration C of the diffusing species in the binary mixture is very less in comparison to the other chemical species, which are present, and hence the Soret and Dufour effects are negligible. Then, under the above assumptions, in the absence of an input electric field, the governing boundary layer equations with Boussinesq's approximation and followed by Makanda *et al*. (2015) are

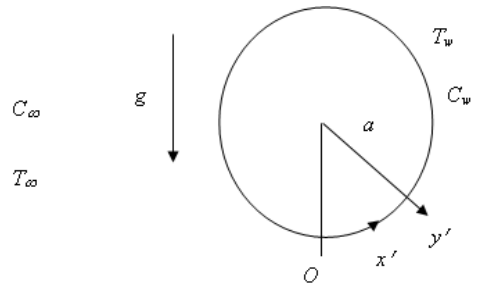

Fig. 1. Flow model and the coordinate system.

$$\frac{\partial u'}{\partial x'} + \frac{\partial v'}{\partial y'} = 0 \tag{1}$$

$$\frac{\partial u'}{\partial t'} + u'\frac{\partial u'}{\partial x'} + v'\frac{\partial u'}{\partial y'} = g\,\beta(T - T_\infty)\sin\left(\frac{x'}{a}\right) + g\,\beta^*(C' - C'_\infty)\sin\left(\frac{x'}{a}\right) + \nu\frac{\partial^2 u'}{\partial y'^2} - \frac{\sigma B_0^2}{\rho}u' \tag{2}$$

$$\frac{\partial T}{\partial t'} + u'\frac{\partial T}{\partial x'} + v'\frac{\partial T}{\partial y'} = \alpha\frac{\partial^2 T}{\partial y'^2} - \frac{1}{\rho c_p}\frac{\partial q_r}{\partial y'} \tag{3}$$

$$\frac{\partial C}{\partial t'} + u'\frac{\partial C}{\partial x'} + v'\frac{\partial C}{\partial y'} = D\frac{\partial^2 C}{\partial y'^2} - K_1(C - C_\infty) \tag{4}$$

The initial and boundary conditions are

$$\begin{aligned} &t' \le 0 : u' = 0, v' = 0,\ T = T_\infty,\ C = C_\infty \\ &t' > 0 : u' = 0, v' = 0,\ T = T_w,\ C = C_w \ \ at\ \ y' = 0 \\ &\qquad u' = 0,\ v' = 0,\ T = T_\infty,\ C = C_\infty \ \ at\ \ x' = 0 \\ &\qquad u' \to 0,\ T \to T_\infty,\ C \to C_\infty \ \ as\ \ y' \to \infty \end{aligned} \tag{5}$$

By using the Rosseland approximation (Brewster [1992]), the radiative heat flux q_r is given by

$$q_r = -\frac{4\sigma_s}{3k_e}\frac{\partial T^4}{\partial y'} \tag{6}$$

It should be noted that by using the Rosseland approximation, the present analysis is limited to optically thick fluids. If the temperature differences within the flow are sufficiently small, then the Eq. (6) can be linearized by expanding T^4 into the Taylor series about T_∞, which after neglecting higher order terms takes the form

$$T^4 \cong 4T_\infty^3\ T - 3T_\infty^4 \tag{7}$$

In view of the Eqs. (6) and (7), the Eq. (3) reduces to

$$\frac{\partial T}{\partial t'} + u'\frac{\partial T}{\partial x'} + v'\frac{\partial T}{\partial y'} = \alpha\frac{\partial^2 T}{\partial y'^2} + \frac{16\sigma_s T_\infty^3}{3k_e\rho c_p}\frac{\partial^2 T'}{\partial y'^2} \tag{8}$$

From technological point of view, it is important to calculate the skin friction, Nusselt number and Sherwood number.

Local and average skin-friction, heat and mass transfer rates are given respectively by

$$\tau_x = -\mu\left(\frac{\partial u'}{\partial y'}\right)_{y'=0} \qquad \bar{\tau} = \frac{-1}{a}\int_0^a \mu\left(\frac{\partial u'}{\partial y'}\right)_{y'=0} dx' \tag{9}$$

$$Nu_x = \frac{-x'\left(\frac{\partial T}{\partial y'}\right)_{y'=0}}{T_w - T_\infty} \qquad \overline{Nu} = -\int_0^a \frac{\left(\frac{\partial T}{\partial y'}\right)_{y'=0}}{(T_w - T_\infty)}dx' \tag{10}$$

$$Sh_x = \frac{-x'\left(\frac{\partial C}{\partial y'}\right)_{y'=0}}{C_w - C_\infty}, \qquad \overline{Sh} = -\int_0^a \frac{\left(\frac{\partial C}{\partial y'}\right)_{y'=0}}{(C_w - C_\infty)}dx' \tag{11}$$

In order to write the governing equations and the boundary conditions in dimensionless form, the following non-dimensional quantities are introduced.

$$X = \frac{x'}{a}, Y = \frac{y'Gr^{1/4}}{a}, t^1 = \frac{ta^2}{\nu}Gr^{-1/2},$$
$$u = \frac{u'aGr^{-1/2}}{\nu}, v = \frac{v'aGr^{-1/4}}{\nu}$$
$$Gr = \frac{g\beta a^3(T_w - T_\infty)}{\nu^2}, \; Gc = \frac{g\beta^* a^3(C_w - C_\infty)}{\nu^2},$$
$$R = \frac{k_e k}{4\sigma_s T_\infty^3} M = \frac{\sigma B_0^2 a^2}{\rho\nu Gr^{1/2}},$$
$$\theta = \frac{T - T_\infty}{T_w - T_\infty}, \phi = \frac{C - C_\infty}{C_w - C_\infty}, \Pr = \frac{\nu}{\alpha}, Sc = \frac{\nu}{D},$$
$$N = \frac{\beta^*(C_w - C_\infty)}{\beta(T_w - T_\infty)}, Kr = \frac{K_1 a^2}{\nu Gr^{1/2}} \tag{12}$$

In view of the Eq. (12), the Eqs. (1), (2), (8) and (4) are reduced to the following non-dimensional form

$$\frac{\partial u}{\partial X} + \frac{\partial v}{\partial Y} = 0 \tag{13}$$

$$\frac{\partial u}{\partial t} + u\frac{\partial u}{\partial X} + v\frac{\partial u}{\partial Y} = \frac{\partial^2 u}{\partial Y^2} + (\theta + N\phi)\sin X - Mu \tag{14}$$

$$\frac{\partial \theta}{\partial t} + u\frac{\partial \theta}{\partial X} + v\frac{\partial \theta}{\partial Y} = \frac{1}{\Pr}\left(1 + \frac{4}{3R}\right)\frac{\partial^2 \theta}{\partial Y^2} \tag{15}$$

$$\frac{\partial \phi}{\partial t} + u\frac{\partial \phi}{\partial X} + v\frac{\partial \phi}{\partial Y} = \frac{1}{Sc}\frac{\partial^2 \phi}{\partial Y^2} - Kr\phi \tag{16}$$

The corresponding initial and boundary conditions are

$$\begin{aligned} &t \le 0 : u = 0, \; v = 0, \; \theta = 0, \; \phi = 0 \\ &t > 0 : u = 0, \; v = 0, \; \theta = 1, \; \phi = 1 \quad at \; Y = 0 \\ &\qquad u = 0, \; v = 0, \; \theta = 0, \; \phi = 0 \quad at \; X = 0 \\ &\qquad u \to 0, \; \theta \to 0, \; \phi \to 0 \quad as \; Y \to \infty \end{aligned} \tag{17}$$

The dimensionless local and average skin-friction, Nusselt number and Sherwood numbers are

$$\tau_x = Gr^{3/4}\left(\frac{\partial u}{\partial Y}\right)_{Y=0}, \quad \bar{\tau} = Gr^{3/4}\int_0^1 \left(\frac{\partial u}{\partial Y}\right)_{Y=0} dX \tag{18}$$

$$Nu_x = -XGr^{1/4}\left(\frac{\partial \theta}{\partial Y}\right)_{Y=0}, \overline{Nu} = -Gr^{1/4}\int_0^1 \left(\frac{\partial \theta}{\partial Y}\right)_{Y=0} dX \tag{19}$$

$$Sh_x = -XGr^{1/4}\left(\frac{\partial \phi}{\partial Y}\right)_{Y=0}, \overline{Sh} = -Gr^{1/4}\int_0^1 \left(\frac{\partial \phi}{\partial Y}\right)_{Y=0} dX \tag{20}$$

3. SOLUTION OF THE PROBLEM

An implicit finite difference scheme of Crank-Nicolson type is employed to solve the non-linear coupled Eqs. (13) - (16), under the boundary conditions (19). The region of integration is considered as a rectangle with sides X_{max} (= $\pi/2$) and Y_{max} (= 14), where Y_{max} corresponds to $Y = \infty$, which lies very well outside the momentum, energy and concentration boundary layers. The maximum of Y was chosen as 14 after some preliminary investigations so that the last two of the boundary conditions of Eq. (17) are satisfied with in the tolerance limit 10^{-5}.

The finite difference equations corresponding to the dimensionless governing partial differential Eqs. (13) - (16) are as follows

$$\frac{\left[u_{i,j}^{n+1} - u_{i-1,j}^{n+1} + u_{i,j}^{n} - u_{i-1,j}^{n} + u_{i,j-1}^{n+1} - u_{i-1,j-1}^{n+1} + u_{i,j-1}^{n} - u_{i-1,j-1}^{n}\right]}{4\Delta X} + \frac{\left[v_{i,j}^{n+1} - v_{i,j-1}^{n+1} + v_{i,j}^{n} - v_{i,j-1}^{n}\right]}{2\Delta Y} = 0 \tag{21}$$

$$\frac{\left[u_{i,j}^{n+1} - u_{i,j}^{n}\right]}{\Delta t} + u_{i,j}^{n}\frac{\left[u_{i,j}^{n+1} - u_{i-1,j}^{n+1} + u_{i,j}^{n} - u_{i-1,j}^{n}\right]}{2\Delta X} + v_{i,j}^{n}\frac{\left[u_{i,j+1}^{n+1} - u_{i,j-1}^{n+1} + u_{i,j+1}^{n} - u_{i,j-1}^{n}\right]}{4\Delta Y} = \left(\frac{\left[\theta_{i,j}^{n+1} + \theta_{i,j}^{n}\right]}{2} + N\frac{\left[\phi_{i,j}^{n+1} + \phi_{i,j}^{n}\right]}{2}\right)\sin X + \frac{\left[u_{i,j-1}^{n+1} - 2u_{i,j}^{n+1} + u_{i,j+1}^{n+1} + u_{i,j-1}^{n+1} - 2u_{i,j}^{n} + u_{i,j+1}^{n}\right]}{2(\Delta Y)^2} - M\frac{\left[u_{i,j}^{n+1} + u_{i,j}^{n}\right]}{2} \tag{22}$$

$$\frac{[\theta_{i,j}^{n+1} - \theta_{i,j}^{n}]}{\Delta t} + u_{i,j}^{n}\frac{\left[\theta_{i,j}^{n+1} - \theta_{i-1,j}^{n+1} + \theta_{i,j}^{n} - \theta_{i-1,j}^{n}\right]}{2\Delta X} + v_{i,j}^{n}\frac{\left[\theta_{i,j}^{n+1} - \theta_{i,j-1}^{n+1} + \theta_{i,j+1}^{n} - \theta_{i,j-1}^{n}\right]}{4\Delta Y} = \frac{1}{\Pr}\left(1 + \frac{4}{3R}\right)\frac{\left[\theta_{i,j-1}^{n+1} - 2\theta_{i,j}^{n+1} + \theta_{i,j+1}^{n+1} + \theta_{i,j-1}^{n} - 2\theta_{i,j}^{n} + \theta_{i,j+1}^{n}\right]}{2(\Delta Y)^2} \tag{23}$$

$$\frac{[\phi_{i,j}^{n+1} - \phi_{i,j}^{n}]}{\Delta t} + u_{i,j}^{n}\frac{\left[\phi_{i,j}^{n+1} - \phi_{i-1,j}^{n+1} + \phi_{i,j}^{n} - \phi_{i-1,j}^{n}\right]}{2\Delta X} + v_{i,j}^{n}\frac{\left[\phi_{i,j+1}^{n+1} - \phi_{i,j-1}^{n+1} + \phi_{i,j+1}^{n} - \phi_{i,j-1}^{n}\right]}{4\Delta Y} = \frac{1}{Sc}\frac{\left[\phi_{i,j-1}^{n+1} - 2\phi_{i,j}^{n+1} + \phi_{i,j+1}^{n+1} + \phi_{i,j-1}^{n} - 2\phi_{i,j}^{n} + \phi_{i,j+1}^{n}\right]}{2(\Delta Y)^2} - Kr\frac{\left[\phi_{i,j}^{n+1} + \phi_{i,j}^{n}\right]}{2} \tag{24}$$

An appropriate mesh sizes considered for the calculation are $\Delta X = 0.05$, $\Delta Y = 0.25$, and the time step $\Delta t = 0.01$. During any one time step, the coefficients $U^n_{i,j}$ and $V^n_{i,j}$ appearing in the difference equations are treated as constants. The values of ϕ, θ, u and v at time level $(n+1)$ using the known values at previous time level (n) are calculated as follows.

The finite difference Eq. (24) at every internal nodal point on a particular i-level constitutes a tridiagonal system of equations. The resultant system of equations is solved using Thomas algorithm as discussed in Carnahan *et al.* (1969). Thus, the values of ϕ are known at every internal nodal point on a particular i at $(n+1)^{th}$ time level. Similarly, the values of $\theta$are calculated from the Eq. (23). Using the values of ϕ and θat $(n+1)^{th}$ time level in the Eq. (22), the values of u at $(n+1)^{th}$ time level are found in similar manner. Thus the values of ϕ, θ and u are known on a particular i-level. Then the values of v are calculated explicitly using the Eq. (21) at every nodal point at particular i-level at $(n+1)^{th}$ time level. This process is repeated for various i-levels. Thus the values of ϕ, θ, u and v are known, at all grid points in the rectangular region at $(n+1)^{th}$ time level.

Computations are carried out until the steady state is reached. The steady-state solution is assumed to have been reached, when the absolute difference between the values of u as well as temperature θ and concentration ϕ at two consecutive time steps are less than 10^{-5} at all grid points. The derivatives involved in the Eqs. (21) to (24) are evaluated using five-point approximation formula and the integrals are evaluated using Newton-Cotes closed integration formula. The truncation error in the finite difference approximation is $O(\Delta t^2 + \Delta Y^2 + \Delta X)$ and it tends to zero as Δt, ΔY, $\Delta X \to 0$. Hence the scheme is compatible. The finite-difference scheme is unconditionally stable as explained by Ganesan and Rani (1998). Stability and compatibility ensures convergence. The derivatives involved in the Eqs. (18) - (20) are evaluated using five-point approximation formula and then the integrals are evaluated using Newton-Cotes closed integration formula.

5. RESULTS AND DISCUSSION

In order to get a physical insight into the problem, a representative set of numerical results is obtained and shown graphically in Figs. 2-15, to illustrate the influence of physical parameters on the velocity, temperature, concentration as well as the skin-friction, Nusselt number and Sherwood number. Here the value of Pr is chosen as 0.7, which represents air. The value of Sc is chosen such that it represents Helium (0.2). The other parameters are chosen arbitrarily. In all the figures * indicates the steady state values.

In order to validate the present results obtained by Crank-Nicolson finite difference method, the transient velocity profiles versus Y at X=1.0 and the steady state local skin friction distributions versus the axial co-ordinate X, for various combinations of Pr, Sc, Kr and N are compared with the computations of Network Simulation Method of Palani and Sreekanth (2009) and shown in Fig. 2. It is found that there is an excellent agreement.

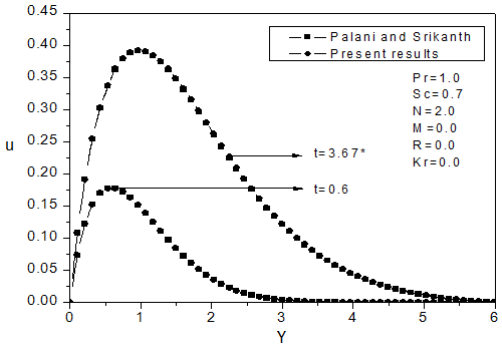

Fig. 2. Comparison of the velocity profiles at X = 1.0.

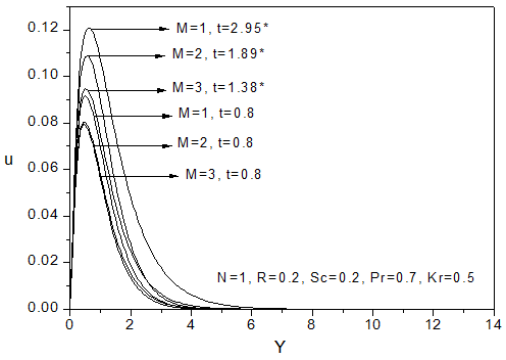

Fig. 3. Transient velocity profiles at $X = \pi/2$ for different M.

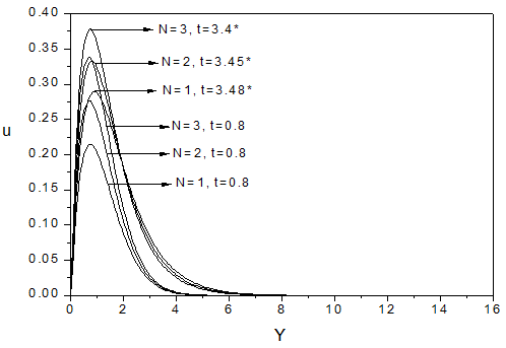

Fig. 4. Transient velocity profiles at $X = \pi / 2$ for different N.

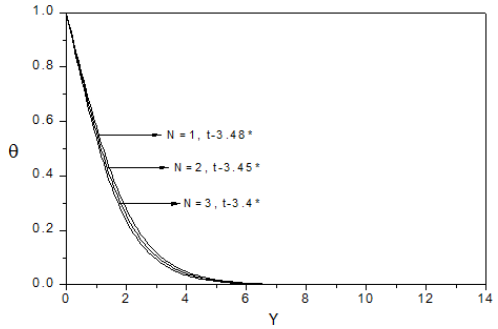

Fig. 5. Effect of N on the steady state temperature at $X = \pi/2$.

Transient velocity profiles on the magnetic parameter *M* is illustrated in Fig. 3. It is observed that the velocity decreases with an increase in the magnetic parameter. The magnetic parameter retards the velocity at all points of the flow field because the application of transverse magnetic field will result in a resistive type force (Lorentz force) similar to drag force which in turn impedes the motion of the fluid flow and thus reducing its velocity. The effect of the buoyancy ratio parameter *N* on the transient velocity is displayed in Fig. 4. It is noticed that the velocity increases with an increase in the values of the buoyancy ratio parameter.

Fig. 5 shows the distribution of steady state temperature against *Y* for various buoyancy ratio parameter *N* values. It is observed that, with an increase in *N*, the thickness of the thermal boundary layer decreases and there will be a corresponding uniformity of temperature distributions across the boundary layer.

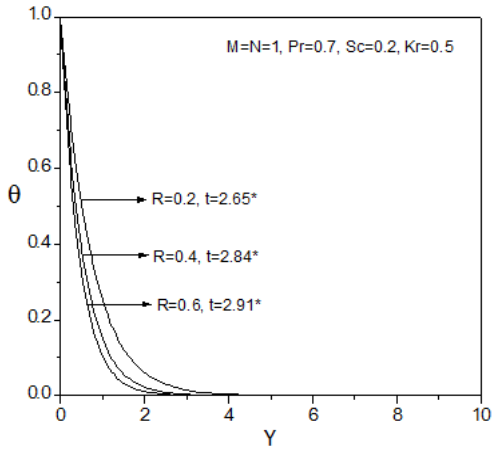

Fig. 6. Effect of *R* on the steady state temperature at $X = \pi/2$.

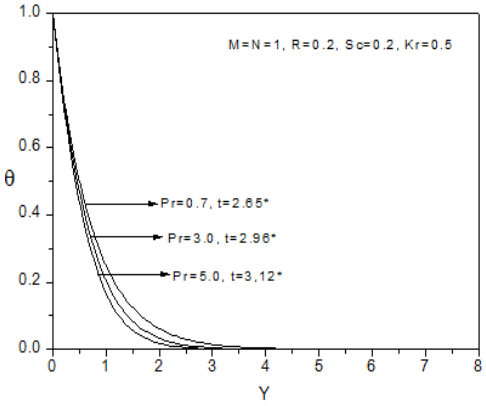

Fig. 7. Effect of *Pr* on the steady state temperature at $X = \pi/2$.

The effect of radiation parameter *R* on the steady state temperature is portrayed in Fig. 6. It is observed that a rise in the radiation parameter leads to a fall in the temperature. As the radiation parameter defines the ratio of the thermal conduction relative to the thermal radiation, the increase in the radiation parameter decreases the thermal radiation, and hence decreases the temperature at large values of *R*. Fig. 7 shows the distribution of temperature against *Y* for various values of the Prandtl number. It is noticed that with an increase in *Pr*, the thickness of the thermal boundary layer decreases and there will be a corresponding uniformity of temperature distributions across the boundary layer. It is seen that the maximum temperature corresponds to lower *Pr* values. The profiles also steepen and intersect the abscissa faster for higher *Pr* fluids i.e. temperature across the boundary layer (normal to wall) reaches to zero rapidly.

Fig. 8 depicts the distribution of concentration against *Y* for various values of Schmidt number *Sc*. It is found that with an increase in *Sc*, the thickness of the concentration boundary layer decreases and there will be a corresponding uniformity of concentration distributions across the boundary layer. The effect of the chemical reaction parameter *Kr* on the steady state concentration is displayed in Fig. 9. In the present study, a homogeneous first-order chemical reaction is considered. Hence, the chemical reaction parameter *Kr* has the dimensions of the reciprocal of time. It is noticed that the concentration decreases with increasing values of the chemical reaction parameter.

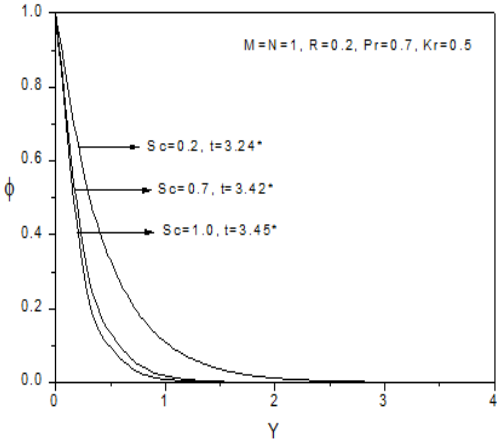

Fig. 8. Concentration profiles for different *Sc* at $X = \pi/2$.

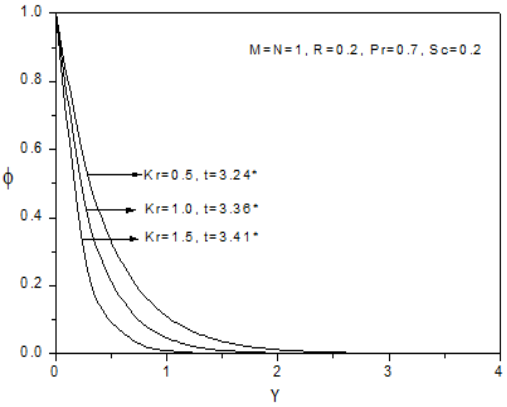

Fig. 9. Concentration profiles for different *Kr* at $X = \pi/2$.

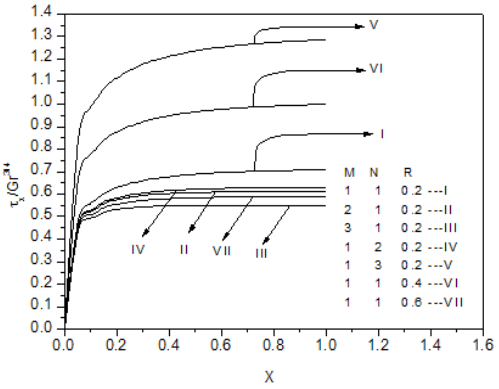

Fig. 10. The local skin friction for different values of *M, N* and *R*.

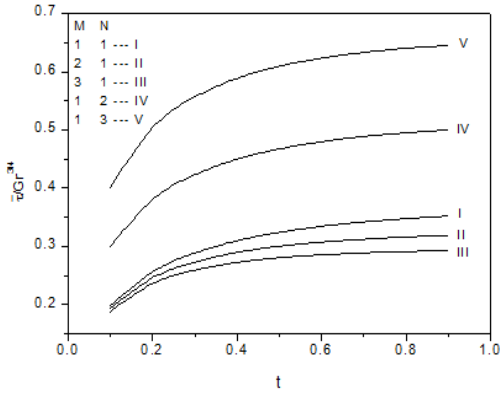

Fig. 11. The average skin friction for different *M* and *N*.

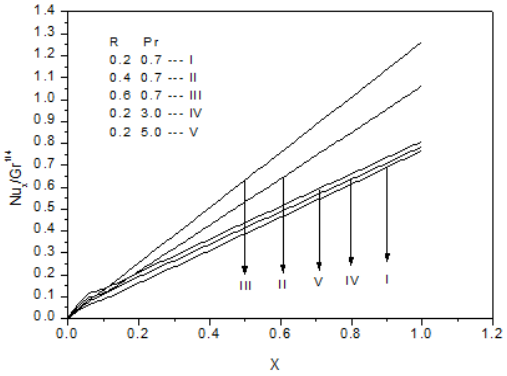

Fig. 12. The local Nusselt number for different *R* and *Pr*.

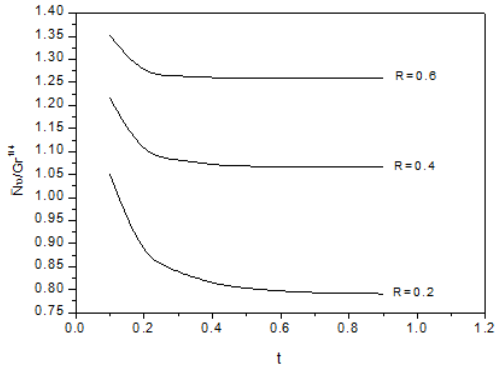

Fig. 13. Effect of *R* on the average Nusselt number.

Fig. 10 illustrates the effects of the magnetic parameter *M,* buoyancy ratio parameter *N* and radiation parameter *R* on the local skin-friction. The local skin-friction is found to decrease due to an increase in the magnetic field strength or radiation parameter *R*. An increase in *N* produces an increase in the local skin-friction. The effects *M* and *N* on the average skin-friction are shown in Fig. 11. It is observed that the average skin-friction increases as *N* increases, and it decreases as *M* increases. Figs. 12 shows the effects of *R* and *Pr* on the local Nusselt number. It is noticed that the local Nusselt number increases as *R* increases and it decreases as *Pr* increases. The effect of *R* on the average Nusselt number is shown in Fig. 13.It is clear that an increase in *R* leads to an increase in the average Nusselt number. Figs. 14 and 15 display the effects of *Sc* and *Kr* on the local and average Sherwood numbers, respectively. It is observed that as *Sc* or *Kr* increases the local and average Sherwood numbers increase.

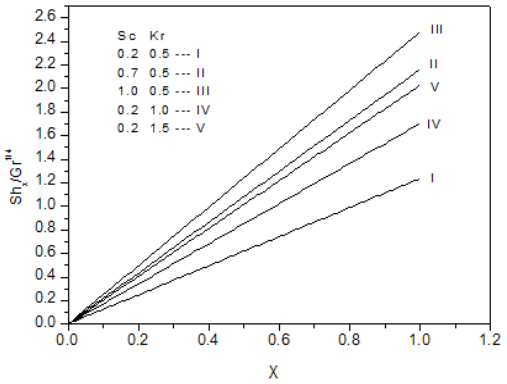

Fig. 14. The local Sherwood number for different *Sc* and *Kr*.

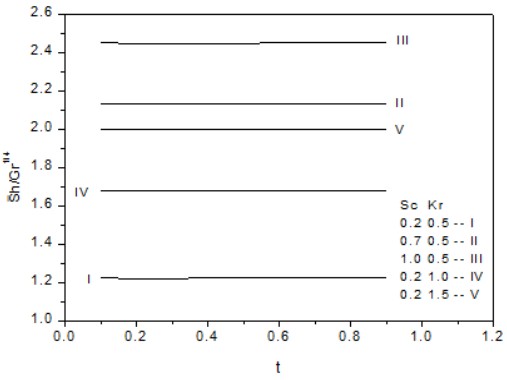

Fig. 15. The average Sherwood number for different *Sc* and *Kr*.

6. CONCLUSIONS

The effects of thermal radiation, chemical reaction, heat and mass diffusion on a mixed convection flow over a horizontal circular cylinder have been investigated. The equations of continuity, linear momentum, energy and diffusion, which govern the flow field, are solved by an implicit finite difference method of Crank-Nicolson type. From the present

investigation the following conclusions may be drawn:

- Each of the transient velocity, temperature and concentration profiles reach to a maximum value before decreasing slightly to their respective steady-state value.
- Velocity increases with an increase in the buoyancy ratio parameter or magnetic parameter.
- An increase in the buoyancy ratio parameter or radiation parameter or Prandtl number decreases the temperature of the fluid.
- The species concentration decreases with an increase in the Schmidt number or chemical reaction parameter.
- Local and average skin friction coefficients decrease with an increase in *M*.
- The local and average Nusselt numbers increase with an increase in *R*.
- As the chemical reaction parameter *kr* increases, the local and average sherwood numbers increase.

REFERENCES

Aboeldahab, E. M. and M. A. Seddeek (2001). Radiation effects on unsteady MHD free convection with Hall current near an infinite vertical porous plate. Intl. *J. Math. Math. Sci. 26, 249-255.*

Bhuiyan, A. S., N. H. M. A. Azim and M. K. Chowdhury (2014). Joule heating effects on MHD natural convection flows in presence of pressure stress work and viscous dissipation from a horizontal circular cylinder. *Journal of Applied Fluid Mechanics* 7(1), 7-13.

Brewster, M. Q. (1992). Thermal radiative transfer properties, Wiley, New York, USA.

Carnahan, B., H. A. Luther and J. O. Willkes (1969). *Applied Numerical Methods*, John Wiley *and* Sons, New York.

Das, S., R. N. Jana and A. J. Chamkha (2015). Unsteady free convection flow past a vertical plate with heat and mass fluxes in the presence of thermal radiation. *Journal of Applied Fluid Mechanics 8(40), 845-854*.

Das, U. N., R. K. Deka and V. M. Soundalgekar (1994). Effects of mass transfer on flow past an impulsively started infinite vertical plate with constant heat flux and chemical reaction. *Forschung imIngenieurwesen 60(10), 284-290.*

Elbashbeshy, E. M. A. (2000). Radiation effect on heat transfer over a stretching surface. *Can. J. Phys. 78, 1107-1112.*

Elbashbeshy, E. M. A. and D. A. Aldawody (2011). Effects of thermal radiation and magnetic field on unsteady mixed convection flow and heat transfer over a porous stretching surface in the presence of internal heat generation/absorption. *International Journal of the Physical Sciences 6(6), 1540-1548.*

El-Hakiem, M. A. and A. M. Rashad (2007). Effect of radiation on non-Darcy free convection from a vertical cylinder embedded in a fluid-saturated porous medium with a temperature-dependent viscosity. *J. Porous Media 10, 209-218.*

Ganesan, P. and H. P. Rani (2000). On diffusion of chemically reactive species in convective flow along a vertical cylinder. *Chemical Engineering and Processing 39, 93-105.*

Ganesan, P. and P. Loganathan (2002). Heat and mass flux effects on a moving vertical cylinder with chemically reactive species diffusion. *Journal of Engineering Physics and Thermophysics 75, 899-909.*

Ganesan, P. and P. Loganathan (2005). Radiation and mass transfer effects on flow of an incompressible viscous fluid past a moving vertical cylinder. *International Journal of Heat and Mass Transfer 45, 4281-4288.*

Ghaly A. Y. and E. M. A. Elbarbary (2000). Radiation effect on MHD free-convection flow of a gas as a stretching surface with a uniform free stream. *J. Appl. Math. 2, 93-103*.

Gilbert, M., S. Sachin and S. Precious (2015). Effects of radiation on MHD free convection of a Casson fluid from a horizontal circular cylinder with partial slip in non-Darcy porous medium with viscous dissipation. Boundary Value Problems *75.*

Goldstein, R. J. and D. G. Briggs (1964). Transient free convection about a vertical plates and circular cylinders, Trans. *ASME C. J. Heat transfer 86, 490-500.*

Hamzeh Duwair, M. (2006). Radiation Effects on Mixed Convection over a Nonisothermal Cylinder and Sphere in a Porous Media *Journal of Porous Media 9(3), 251-259*.

Hossain, M. A., M. Kutibuddin and H. S. Tarkar (1999). Radiation interaction on combined forced and free convection across a horizontal cylinder. *International Journal of Applied Mechanics and Engineering 4, 219-235.*

Loganathan, P., M. Kannan and P. Ganesan (2011). Thermal radiation effects on MHD flow over a moving semi-infinite vertical cylinder. *Int. Journal of Math. Analysis 5(6), 257-274.*

Md Hye, A., M. D. M. Molla and M. A. H. Khan (2007). Conjugate effects of heat and mass transfer on natural convection flow across an isothermal horizontal circular cylinder with chemical reaction. *Nonlinear Analysis: Modeling and Control 12(2), 191-201.*

Molla, M. M., S. C. Saha, M. A. I. Khan and M. A. Hossain (2011). Radiation effects on natural convection laminar flow from a horizontal circular cylinder. *Desalination and Water Treatment 30*, 89-97.

Muthucumaraswamy, R. and M. Ravi Shankar (2004). First order chemical reaction and thermal radiation effects on unsteady flow past an accelerated isothermal infinite vertical plate. *Indian Journal of Science and Technology 4, 573-577*.

Palani, G. and U. Srikanth (2009). MHD flow past a semi-Infinite vertical plate with mass transfer. *Nonlinear Analysis: Modeling and Control 14(3), 345-356.*

Rahman, M. M., M. A. H. Mamun, R. Saidur and N. Shuichi (2009). Effect of a heat conducting horizontal circular cylinder on MHD mixed convection in a lid-driven cavity along with joule heating *International Journal of Mechanical and Materials Engineering (IJMME) 4(3), 256-265.*

Seddeek, M. A. (2001). Thermal radiation and buoyancy effects on MHD free convective heat generating flow over an accelerating permeable surface with temperature-dependent viscosity. *Can. J. Phys. 79, 725-732.*

Shit, G. C. and S. Majee (2014). Hydromagnetic flow over an inclined non-linear stretching sheet with variable viscosity in the presence of thermal radiation and chemical reaction. *Journal of Applied Fluid Mechanics 7(2), 239-247.*

Sreenivasulu, P. and N. Bhaskar Reddy (2015). Lie Group analysis for boundary layer flow of nanofluids near the stagnation-point over a permeable stretching surface embedded in a porous medium in the presence of radiation and heat generation/absorption. *Journal of Applied Fluid Mechanics 8(3), 549-558*.

Ziya, U. and M. Kumar (2011). MHD heat and mass transfer free convection flow near the lower stagnation point of an isothermal cylinder imbedded in porous domain with the presence of radiation, *Jordan Journal of Mechanical and Industrial Engineering 5(2), 133-138.*